TERASAKI INSTITUTE FOR BIOMEDICAL INNOVATION

11570 W Olympic Blvd, Los Angeles, CA 90064

Thermoresponsive Shear-Thinning Hydrogel (T-STH) Hemostats for Minimally Invasive Treatment of External Hemorrhages

Abstract: Hemorrhage is the leading cause of death following battlefield injuries. Although several hemostats are commercially available, they do not meet all the necessary requirements to stop bleeding in combat injuries. Here, we engineer thermoresponsive shear-thinning hydrogels (T-STH) as minimally invasive injectable hemostatic agents. Our T-STH can be easily injected through a syringe and needle and exhibits rapid mechanical recovery. Additionally, it demonstrates temperature-dependent blood coagulation, decreases in vitro blood clotting times over 50%, and significantly prevents blood loss in an ex vivo bleeding model at different blood flow rates. More importantly, our T-STH is comparable to a commercially available hemostat, Floseal, in an in vivo rat liver bleeding model. Furthermore, once the hemorrhage is stabilized, our T-STH can be easily removed using a cold saline wash without any rebleeding or leaving any residues.

Schematic illustration and phase transition

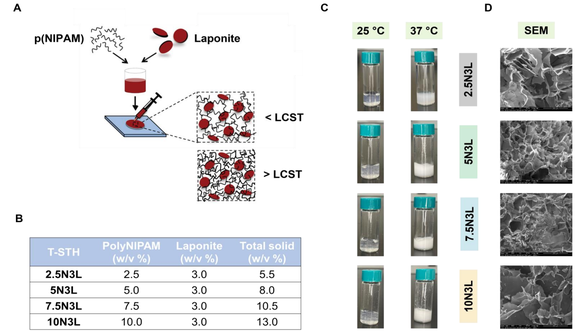

T-STH	PolyNIPAM (w/v %)	Laponite (w/v %)	Total solid (w/v %)
2.5N3L	2.5	3.0	5.5
5N3L	5.0	3.0	8.0
7.5N3L	7.5	3.0	10.5
10N3L	10.0	3.0	13.0

Fig. 1 | (A) Schematic showing the preparation of our T-STH as an injectable hemostat for hemorrhage control. (B) Table summarizing the compositions of our T-STH formulations. (C) Representative images of our T-STH at 25 ℃ and at 37 ℃. (D) Representative SEM images of our p(NIPAM) and Laponite-based T-STH.

In vitro clotting studies

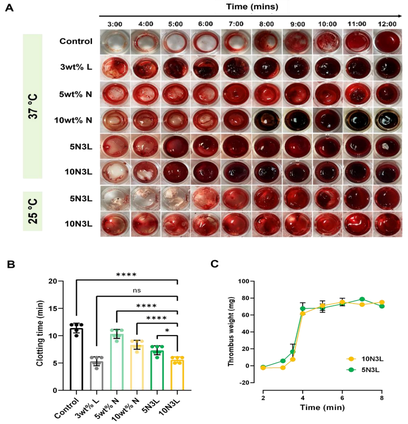

Fig. 2 | (A) 48-well plate assay of blood clotting in contact with control (polystyrene substrate), Laponite control (3 w/v %), p(NIPAM) control (5 w/v % and 10 w/v %), and our T-STH. Our T-STHs show temperature-dependent blood coagulation. (B) Quantitative clotting times as determined by the 48-well plate assay. (C) Time series of clot formation by measuring the thrombus weight of our T-STHs.

Ex vivo bleeding flow model

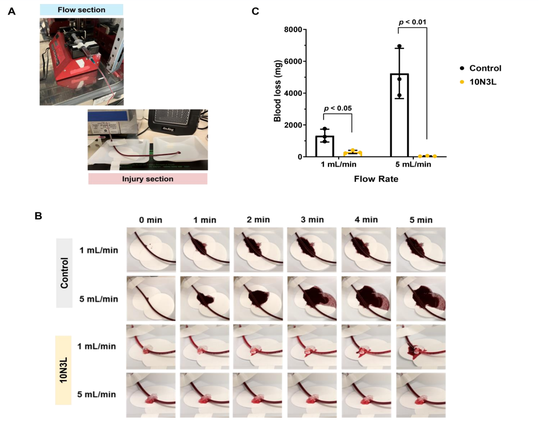

Fig. 3 | (A) Experimental setup of the *ex vivo* bleeding model with the "flow" section housed within a 37 ℃ incubator, and the "injury" section placed outside the incubator on a heating pad set at 37 ℃. (B) Representative images of blood loss from an "injury" created by a 1.5 mm biopsy punch. 10N3L can create a plug at the "injury" site and prevent blood loss. (C) Quantitative blood loss (mg) from the "injury" after 5 mins.

In vivo liver bleeding model

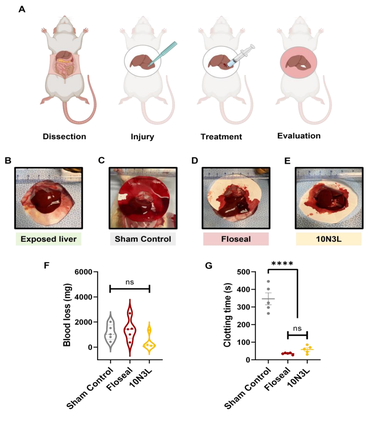

Fig. 4 | (A) Schematic of the *in vivo* bleeding model prepared using BioRender. The rat was dissected, and the liver was exposed (B) and placed on a Whatman weighing paper. A biopsy punch (4 mm) was used to create and injury in the lower right lobe, and the wound was treated with three groups (n = 5): sham control (negative control), Floseal (commercial positive control), and T-STH. Representative images of the bleeding liver after treatment with either (C) sham control, (D) Floseal, and (E) 10N3L. The (F) clotting time, and (G) blood loss from the wound after treating with the hemostatic materials.

Conclusions

Our T-STHs formed injectable biomaterials that could be easily administered via a syringe, had higher G' values at physiological temperatures, were hemo- and cytocompatible, and promoted temperature-dependent *in vitro* coagulation. They significantly reduced blood loss in an *ex vivo* model from two different blood flow rates (1 and 5 mL/min), and was comparable to a commercially available hemostat, Floseal, in an *in vivo* rat bleeding model in terms of blood loss and clotting time. Moreover, they are mechanically stable under physiological conditions, accelerate local hemostasis without any clotting factors, and can be easily removed using a cold saline wash without leaving any residues. This works paves the way for a new class of thermoresponsive hemostats for the treatment of external hemorrhages.

Acknowledgements

This work is supported by the National Institutes of Health (5R01HL137193) and the Terasaki Institute of Biomedical Innovation

Biodegradable and Flexible GelMA Aerogel (FGA)-based Electronic Skin for Wearable Multiplexed Physical-Electrophysiological-Chemical Analysis

Abstract: Mimicking the extensive sensing capabilities in humans via electronic skin (E-skin) is essential for assessing the effects of daily routines on the physical, physiological, and metabolic response of the human body, all of which require an E-skin that can simultaneously track metabolic biomarkers and physiological signals. Conventional E-skins built with elastomeric films lack breathability, skin comfortability, thermal management, environmental friendliness, and anti-inflammation activity, which impedes wearing comfort, limits multiplexed device integration, and creates skin irritation and/or inflammation with long-term use. Herein, we report a breathable, passive-cooling, non-inflammatory, biodegradable, and flexible E-skin based on gelatin methacryloyl (GelMA) aerogel for non-invasive and continuous monitoring of body temperature, skin hydration, and biopotentials via electrophysiological sensors, and of multiple biomarkers (glucose, lactate, and alcohol) via electrochemical sensors.

Conceptual illustration of FGA-based E-Skin

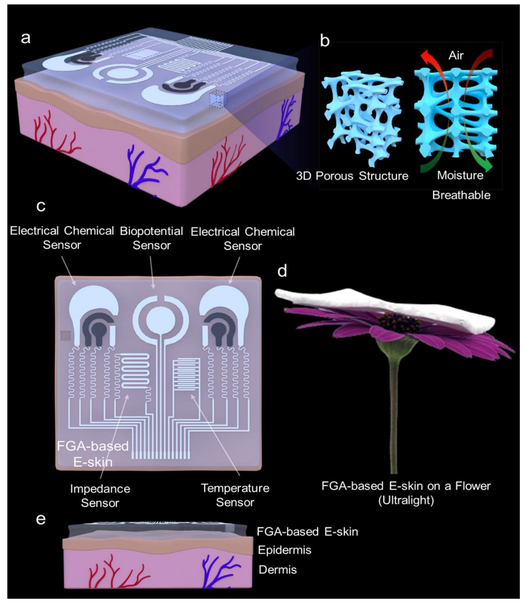

Fig. 1 | a, Application scenario of the integrated FGA-based E-skin that can be attached onto the epidermis. b, Schematic illustration of the three-dimensional porous network structure of the FGA that endows the breathable capabilities. c, Top view of the multiple sensor integrated on aerogel surface including electrochemical sensor, biopotential sensor temperature sensor, and impedance sensor. d, FGA-based E-skin on a flower, indicating its ultra-light weight. e, Side view of the FGA-based E-skin worn on the epidermal surface to suggest the conformal capability of the FGA-based E-skin.

Biocompatibility of FGA-based E-Skin

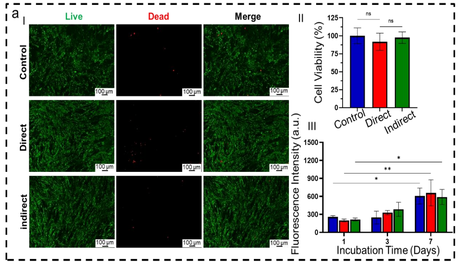

Fig. 2 | a, Fluorescent images of cells cultured in the incubation medium with the FGA. Quantification of human dermal fibroblast cell viability and absorption at 570 nm in 3-(4,5-dimethylthiazol-2-yl)-2,5-diphenyltetrazolium bromide (MTT) assay of FGA after 1, 3 and 7 days of incubation. Error bars show standard deviation.

Acknowledgements

This work is supported by the National Institutes of Health (AR074234, UG3TR003148, GM126571, GM126831).

On-body validation of FGA-based E-Skin

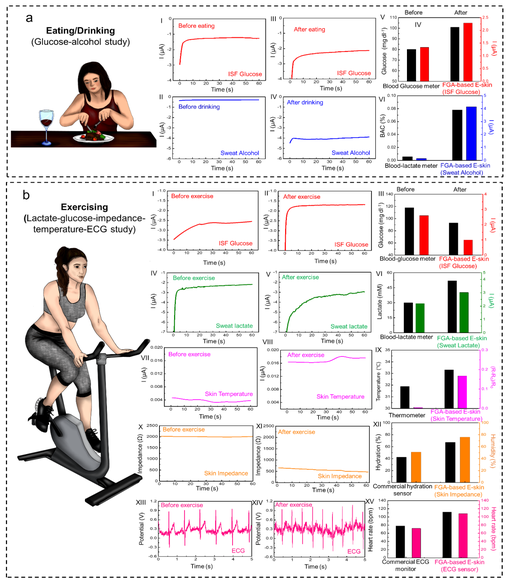

Fig. 3 | a, Multi-event study of the FGA-based E-skin involving food and alcohol consumption events. (I-II), Electrochemical sensor signal recordings for ISF glucose before and after food-intake. (III) Comparison between the glucose levels in interstitial fluid (ISF) measured using the electrochemical sensor and in blood using a blood-glucose meter. (IV-V) Electrochemical sensor signal recordings for sweat alcohol levels before and after wine-intake. (VI) Comparison between the alcohol levels in sweat measured using the FGA-based E-skin and in blood using a commercial blood-lactate meter. b, Multiplexed chemical-electrophysiological analysis during the exercise. (I-II) Electrochemical sensor signal recordings for ISF glucose levels before and after high-intensity exercise. (III) Comparison between the glucose levels in ISF measured using the FGA-based E-skin and in blood using a commercial blood-glucose meter. (IV-V) Electrochemical sensor recordings for sweat lactate levels before and after exercise. (VI) Comparison between the alcohol levels in sweat using the FGA-based E-skin and in blood using a commercial blood-alcohol meter. (VII-VIII) Physiological signal recordings for skin temperature variations before and after exercise. (IX) Comparison between the skin temperature measured using the FGA-based E-skin and commercial thermometer. (X-XI) Physiological signal recordings for skin impedance/hydration levels before and after exercise. (XII) Comparison between the skin impedance/hydration levels measured using the FGA-based E-skin and commercial hydration sensor. (XIII-XIV) Physiological signal recordings for electrocardiogram (ECG) before and after exercise. (XV) Comparison between the heart rate measured using the FGA-based E-skin and commercial ECG monitor.

Conclusions

We have demonstrated a breathable, passive-cooling, biocompatible, biodegradable, and flexible FGA-based E-skin for non-invasive, real-time, and simultaneous monitoring of hybrid chemical-electrophysiological-physical signals. We validated the performance of this aerogel E-skin by monitoring the ISF glucose, lactate and alcohol levels from sweat, skin temperature, impedance/hydration, and ECG patterns as model analytes. This work paves the way for a class of multifunctional aerogel-based electronic skin capable of providing informative data regarding human healthcare and lays the foundation for next-generation, patient-centered diagnostic, and therapeutic tools.